Spatial regionalization as optimal data compression

Alec Kirkley $^{1, 2}$

¹Department of Physics, University of Michigan, Ann Arbor, Michigan 48109, USA ²School of Data Science, City University of Hong Kong, Hong Kong

The process of aggregating areal units into contiguous clusters, known as regionalization, is central to the analysis of spatial data. Regionalization provides a means to reduce the effect of noise or outliers in sampled data, identify socioeconomically homogeneous areas for policy development, and simplify the visualization of data in maps among many other applications. Most existing regionalization methods require a substantial amount of manual input, such as the number of desired regions or a similarity measure among regional populations, which may be desirable for some applications but does not allow us to extract the natural regions defined solely by the data itself. Here we view the problem of regionalization as one of data compression. We define the optimal partition of spatial units with corresponding distributional data as the one that minimizes the description length required to transmit the data, and develop an efficient, parameter-free greedy optimization algorithm to identify this partition. We demonstrate that our method is capable of recovering planted spatial clusters in noisy synthetic distributional data, and that it identifies meaningful ethnoracial boundaries in real demographic data. Using our description length formulation, we find that the information contained in spatial ethnoracial data in metropolitan areas across the U.S. has become more difficult to compress over the period from 1980 to 2010, which reflects the rising complexity of urban segregation patterns of these metros. We identify the increasing overall diversity of these metros as a major contributor to this lower data compressibility, while the spatial scale of ethnoracial clustering does not appear to be a significant factor.

I. INTRODUCTION

From the growth of economies [1] to the systemic segregation of human populations [2] to the environmental adaptation of ecological species [3], many social and natural phenomena manifest themselves in space with high levels of clustering among similar agents or entities. Precisely defining the spatial boundaries of these clusters and observing their evolution can shed light on the fundamental processes driving the dynamics of these systems, aid in the reduction of noise in spatially sampled data [4, 5], and facilitate the identification of regions for spatially targeted policy interventions [6] among numerous other applications. Regionalization methods—techniques to perform spatially constrained clustering by aggregating spatial units—are typically the tools of choice for partitioning spatial data into areas of interest for such analysis. Consequently, regionalization methods have been adapted for applications across fields as diverse as climatology [7], urban sociology [8], hydrology [9], geoecology [10], and political science [11].

Many approaches to regionalization typically require a significant amount of input from the user to adjust various parameters prior to performing the clustering. These tunable parameters can be used to constrain the size or shape of clusters, or to avoid crossing administrative or geographical boundaries [12, 13]. User preferences are also commonly incorporated into regionalization methods through the choice of a similarity or distance function between adjacent regions [14, 15]. Additionally, as is the case with any clustering method, a key factor existing regionalization methods consider is the choice of the number of regions, which is typically fixed by the user [12, 16] but is sometimes determined endogeneously

based on user-defined thresholds for covariates of interest or other heuristics that depend or one's choice of dissimilarity between spatial units [15, 17]. An increased level of user control is desirable for many applications of regionalization, as researchers can ensure that the identified regions are suitable for the task at hand and do not violate any necessary constraints. For example, clusters extracted from regionalization methods may be used to define zones designated for different aspects of urban development, and it may be preferred that these zones do not cross significant geographical or infrastructural boundaries.

In other applications of regionalization, however, such as identifying characteristic scales over which segregation or other socioeconomic phenomena persist [18–21], one may be interested in imposing as few assumptions as possible about how the data clusters into regions, and instead rely on the data itself to naturally define these clusters. We adopt this approach for our method, defining the best partition of a set of spatial units as the one that allows us to optimally compress the information contained in a covariate of interest. We employ the minimum description length concept from information theory [22, 23] to quantify the extent to which a given partition allows for compression of the data. By viewing the problem of regionalization from this perspective, our approach does not require the specification of any free parameters, such as an explicit dissimilarity function between spatial units or a particular value for the number of regions we want the algorithm to return. Our method also takes into account the full distribution of the covariate of interest in each spatial unit, rather than summarizing each local distribution with a single statistic such as its mode. In this way, through regionalization we aim to compress all

of the information contained in the spatial covariate, and rely only on the data itself to accomplish the task.

There are a few existing methods for clustering data without spatial constraints that have a similar motivation as our own. The minimum description length principle has been applied for clustering categorical data [24]. real-valued vector data [25], and other sets of objects [26] in aspatial contexts. In [27], an algorithm for community detection in (aspatial) network data is proposed that identifies the partition minimizing the description length of an encoding of the network. This method differs substantially from our own, however, in that it takes only topological information into account, which is relatively uninformative for planar networks of adjacent spatial regions (as is the case in regionalization). By contrast, our method takes into account both topological information (the adjacency between spatial units) as well as spatial covariates. In [28], a regionalization algorithm is proposed, which, in the same spirit as our own method, uses concepts from information theory to define homogeneous aggregations of spatial units. This method also employs a greedy optimization procedure as we do here, but differs significantly from our method in that it requires the user to specify the desired number of regions and chooses the class of Bregman divergences to measure information loss. The method proposed here, on the other hand, allows the user to automatically learn the optimal number of clusters from the data if they choose and uses a simple combinatorial approach to define the information content of a partition.

In this paper we first derive a regionalization objective function based solely on fundamental combinatorial arguments and the minimum description length principle. We then describe a greedy optimization procedure used to obtain a partition that approximately minimizes this description length, which involves iteratively merging the pair of spatial units that maximally reduces the description length. We demonstrate our method on a series of experiments using both real and synthetic spatial data. In the first experiment, we illustrate how our method can effectively recover synthetically planted clusters in spatial distributional data, even in the presence of substantial noise. We move on to show that our method extracts meaningful regions and their evolution in real ethnoracial data by analyzing the New Haven-Milford metropolitan area of the U.S. as a case study, covering the decades between 1980 and 2010. Finally, in an experiment using a set of 110 large metropolitan areas across the U.S., we demonstrate that our method reveals the increasing complexity of urban segregation patterns over this same time period, and that this trend can be well explained by the overall increase in ethnoracial diversity of these metros rather than by the manifestation of clustering at different spatial scales.

II. MATERIALS AND METHODS

A. Description length formulation

We can represent our spatial data to be regionalized as a network G = (V, E) consisting of a set of spatial units (nodes) V and a set of edges E that connect adjacent units. More precisely, the edge $(u,v) \in E$ if and only if units $u \in V$ and $v \in V$ share a length of common border. We denote the number of units in any subset $V' \subseteq V$ of the network as n(V'). Over this set of n(V)units, there are $b(V) \geq n(V)$ individuals residing (we adopt analogous notation for b(V'), and each of these individuals is classified under one of R categories r =1, 2, ..., R. For example, the spatial units u that comprise the network may be census tracts or block groups, and the categories could represent race, income bracket, or occupation type. Our formulation in general will depend on what spatial units are used, and so it is recommended to use regions with the finest granularity possible while also avoiding excessive sampling noise. We also denote with $b_r(V')$ the number of individuals of type r in subset $V' \subseteq V$, such that $\sum_{r=1}^{R} b_r(V') = b(V')$.

Now, suppose we want to transmit to a receiver the entire dataset $D = \{b_r(u) : r = 1, ..., R; u \in V\}$ consisting of the distribution of types r among individuals in all units u. (Since we generally do not know the value r for each individual due to confidentiality concerns, these unit-level distributions are the highest granularity we consider.) We will transmit this data in multiple parts, first partitioning the units u into K disjoint, spatially contiguous clusters $\mathcal{P} = \{V_1, V_2, ..., V_K\}$ that allow us to describe the data to the receiver at a coarse spatial scale. We then transmit the small-scale details within each of these clusters by describing how the cluster's population attributes are distributed among its individual constituent units. Our goal will be to identify a partition \mathcal{P} of the units such that most of the information we need to transmit is contained in the first part, or in other words, that the clusters describe most of the variation in the data and are internally homogeneous.

We assume that the receiver knows there are n(V) units in total that will be assigned to K clusters, and that there are b(V) individuals with R distinct categories that will be assigned to units $u \in V$. (Transmitting these requires a negligible amount of information, so we can safely ignore them in our description length anyway.) We first need to transmit the populations $b(V_k)$ for each of the clusters V_k , which consists of a configuration of K non-negative integer values that sum to b(V). Prior to transmission of the data D, we must develop a common codebook with the receiver, from which we will transmit a binary string representing the particular configuration of the populations $\{b(V_k)\}$. Assuming $K \ll b(V)$, there are approximately $\binom{b(V)-1}{K-1}$ possible configurations of these values, and so we will possibly have to send a bitstring of length $\lceil \log_2 \binom{b(V)-1}{K-1} \rceil$ to the receiver to transmit the

cluster-level populations $\{b(V_k)\}$. $(\lceil x \rceil$ denotes the smallest integer not less than x, and we will omit this transformation in future considerations as its contribution is negligible for $x \gg 1$. For the sake of brevity we will also denote $\log_2(x) \equiv \log(x)$.) Thus, the information content (or "description length") of this step in the transmission procedure is

$$\mathcal{L}(\{b(V_k)\}) = \log \binom{b(V) - 1}{K - 1}.$$
 (1)

Following the same logic, we can construct the description lengths for the rest of the steps required to transmit D according to this scheme. After sending the populations $\{b(V_k)\}$, we must transmit the number of units within each cluster, $\{n(V_k)\}$, for which we will construct a different codebook. This step will have a description length of the same form as Eq. 1, thus

$$\mathcal{L}(\{n(V_k)\}) = \log \binom{n(V) - 1}{K - 1}.$$
 (2)

Now, for each cluster V_k we need to transmit the size distribution $\{b_r(V_k)\}$ of categories within the population $b(V_k)$, which will have the same form as Eq.s 1 and 2. The description length of this step will be a sum over such description lengths, or

$$\mathcal{L}(\{b_r(V_k)\}) = \sum_{k=1}^{K} \log \binom{b(V_k) - 1}{R - 1}.$$
 (3)

Similarly, we need to transmit the populations b(u) of the units $u \in V_k$, for each cluster V_k , which will give a total description length contribution of

$$\mathcal{L}(\{b(u)\}) = \sum_{k=1}^{K} \log \binom{b(V_k) - 1}{n(V_k) - 1}.$$
 (4)

The receiver now knows how many units u are in each cluster V_k , how many individuals are in each of these units, and how categories are distributed across the entire population of V_k . The only information left to transmit is how the categories in each cluster V_k are distributed among the populations in V_k 's constituent units u. The number of ways these values can be distributed is equivalent to the number $\Omega(\boldsymbol{a}_k, \boldsymbol{c}_k)$ of non-negative integer-valued matrices with row sums $\boldsymbol{a}_k = \{b(u)\}_{u \in V_k}$ and column sums $\boldsymbol{c}_k = \{b_r(V_k)\}_{r=1}^R$. We can see this by noting that there are $b(V_k)$ total individuals in cluster V_k , and using the identities

$$b(V_k) = \sum_{u \in V_k} b(u) \tag{5}$$

and

$$b(V_k) = \sum_{r=1}^{R} b_r(V_k).$$
 (6)

The description length for this final step is thus given by

$$\mathcal{L}_{final} = \sum_{k=1}^{K} \log \Omega(\boldsymbol{a}_k, \boldsymbol{c}_k). \tag{7}$$

Computing $\Omega(\boldsymbol{a}_k, \boldsymbol{c}_k)$ is in general challenging, but it can be approximated in the regime $R, n(V_k) \ll b(V_k)$, which is typically the regime we encounter in practice (see Ref. [29] for details on this approximation).

Taken all together, the total description length of the data D is given by the sum of Eq.s 1, 2, 3, 4, and 7, thus

$$\mathcal{L}(D, \mathcal{P}) = \log \binom{b(V) - 1}{K - 1} + \log \binom{n(V) - 1}{K - 1}$$

$$+ \sum_{k=1}^{K} \log \binom{b(V_k) - 1}{R - 1} + \sum_{k=1}^{K} \log \binom{b(V_k) - 1}{n(V_k) - 1}$$

$$+ \sum_{k=1}^{K} \log \Omega(\boldsymbol{a}_k, \boldsymbol{c}_k). \tag{8}$$

We can see that the first three terms in Eq. 8 penalize us for having a greater number of clusters K, as they will tend to contribute greater description lengths as Kincreases. The fourth term will scale like $n(V) \log(b/K)$ for equally sized clusters, and so in general will tend to penalize us slightly for having fewer clusters. In the extreme case where there is only one category r^* that is represented in the population of the units $u \in V_k$ (i.e. $c_k[r] = 0$ for $r \neq r^*$), then we have $\Omega(a_k, c_k) = 1$ and the contribution from the last term in Eq. 8 term vanishes. More generally, there are fewer ways the categories can be distributed among the populations in V_k 's constituent tracts if c_k is more concentrated on a single category, and so the last term in Eq. 8 will penalize us for having a high level of diversity within the clusters. (Or, conversely, this term encourages partitions \mathcal{P} that have homogeneous clusters.)

The optimal partition $\mathcal{P}=\{V_1,...,V_k\}$ that minimizes the description length in Eq. 8 will allow us to communicate most of the information about the data D through the cluster-level distributions alone, but penalize us for constructing these clusters at too small a scale, since this will not save us much effort above and beyond simply transmitting all the unit-level data individually. The goal of our regionalization algorithm is to identify this partition, and we describe an algorithm to accomplish this task in the next section. A diagram of an optimal partition $\mathcal P$ of a synthetic set of example units, along with the variables used in the information transmission scheme, is shown in Fig. 1.

B. Optimization and model selection

Minimization of the description length in Eq. 8, like many other regionalization objectives [12], is a combinatorial optimization problem that can be approached in a

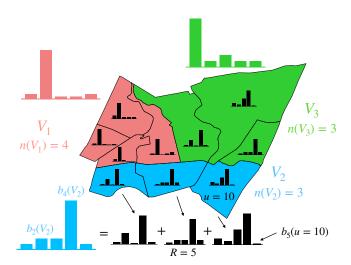


FIG. 1: Diagram of variables in the information transmission process, for the partition \mathcal{P} of the (synthetic) unit-level distributions that gives the minimum description length according to Eq. 8. The optimal partition of this space results in aggregated regions of spatial units that capture most of the information content of the data.

number of ways to obtain an approximate solution. Here, we opt for a greedy solution that consists of starting with each unit in its own cluster then iteratively merging the pair of adjacent clusters whose aggregation results in the largest decrease in Eq. 8, until no merges produce a negative change in the description length. This merging procedure also has the benefit of naturally ensuring that the partition $\mathcal P$ produces only contiguous clusters of units.

For any pair of clusters V_k and $V_{k'}$, we can quickly compute the change in Eq. 8 that results from their aggregation into a single cluster, $V_{k,k'}$. Supposing there are K clusters prior to the proposed merge, the change in description length from merging clusters V_k and $V_{k'}$ is given by

$$\Delta \mathcal{L}(k, k') = \log \begin{pmatrix} b(V_{k,k'}) - 1 \\ R - 1 \end{pmatrix} + \log \begin{pmatrix} b(V_{k,k'}) - 1 \\ n(V_{k,k'}) - 1 \end{pmatrix}$$

$$+ \log \Omega(\boldsymbol{a}_{k,k'}, \boldsymbol{c}_{k,k'}) - \log \begin{pmatrix} b(V_k) - 1 \\ R - 1 \end{pmatrix}$$

$$- \log \begin{pmatrix} b(V_k) - 1 \\ n(V_k) - 1 \end{pmatrix} - \log \Omega(\boldsymbol{a}_k, \boldsymbol{c}_k)$$

$$- \log \begin{pmatrix} b(V_{k'}) - 1 \\ R - 1 \end{pmatrix} - \log \begin{pmatrix} b(V_{k'}) - 1 \\ R - 1 \end{pmatrix}$$

$$- \log \Omega(\boldsymbol{a}_{k'}, \boldsymbol{c}_{k'}).$$

$$(9)$$

Here we have ignored the first two terms in Eq. 8, as these terms change by the same amount across all pairs k, k' and thus do not need to be computed until the optimal pair k, k' is chosen. (Whether or not this pair will be merged or the algorithm will terminate does depend on these first two terms, which can be computed in constant time.) This expression can be evaluated in $O(n(V_k) + n(V_{k'}))$ time for each pair of clusters k, k'. Ad-

ditionally, it only needs to be computed once for each pair of clusters, and can be reused for future iterations of the algorithm if the pair k,k' does not get merged (as long as each newly formed cluster gets a unique label). Once no remaining pair of clusters can be merged to reduce the description length $(\Delta \mathcal{L}(k,k') > 0$ for all adjacent cluster pairs $V_k, V_{k'}$, the algorithm terminates.

The adjacency relations between clusters are updated as the algorithm progress, by merging the neighbor sets of the two clusters that are merged. This takes an additional $O(d_k + d_{k'})$ steps, where d_k is the number of adjacent clusters to cluster k, and is typically much smaller than $O(n(V_k)+n(V_{k'}))$ for large clusters, since many clusters are only adjacent to a few others. We find in practice that the algorithm scales well to large systems, running in much less than order $O(n(V)^2)$ time.

The first few terms in Eq. 8 penalize us for having a large number of clusters, since we waste information describing all of the cluster-level distributions in their entirety. Meanwhile, the last two terms penalize us for having a small number of clusters, since we waste information describing the small scale details of these clusters as they encompass to broad a variety of units. The optimal balance, and thus the optimal value of K, lies somewhere in between with an intermediate number of clusters, and the description length in Eq. 8 thus performs model selection for K automatically. In our example applications, we therefore choose to let the description length tell us exactly how many clusters are in the data. However, in many applications it may be preferable to have a fixed value of K ([12, 26]), and this can easily be accommodated in our algorithm by simply performing the greedy merge moves until there are the desired number of clusters.

We can assess the quality of the information compression achieved through partitioning the units into clusters by comparing the final description length $\mathcal{L}(D,\mathcal{P})$ with the description length $\mathcal{L}(D,\mathcal{P}_0)$ for the trivial partition \mathcal{P}_0 in which each unit is in its own cluster (computed at the beginning of the optimization algorithm). From this we can construct an inverse "compression ratio" for the data D as

$$\eta(D) = \frac{\text{compressed size of } D}{\text{uncompressed size of } D} = \frac{\mathcal{L}(D, \mathcal{P})}{\mathcal{L}(D, \mathcal{P}_0)}.$$
(10)

 $\eta(D)$ approaches its minimum value of 0 when the data D can be compressed extremely efficiently through partitioning, and approaches its maximum value of 1 when there is no partition of the data that achieves any level of information compression. Eq. 10 can thus be used as a measure of the complexity of the spatial segregation of the data D, with more complex spatial distributions of the covariate of interest resulting in higher inverse compression ratios η . Intuitively, if the data D is very easy to compress (low η), then it is highly spatially segregated into homogeneous clusters, and most of the information in D is captured at large scales. On the other hand, if the data is very hard to compress (high η), then much of

the information in the data is manifested at small spatial scales. This could be due to the presence of small-scale segregated clusters or widespread diversity, among numerous other factors that contribute to segregation [30].

C. Ethnoracial data in U.S. metropolitan areas

In addition to synthetic data to examine the performance of our algorithm, we test our method using ethnoracial data that take the form of distributions within census tracts. Ethnoracial distributions for census tracts in U.S. metro areas were obtained from the Longitudinal Tract Database [31], which maps 2010 census tract boundaries to ethnoracial distribution data for decades going back to 1970. (Data from 1970 are omitted from our analysis, as they do not include the designation of Hispanic ethnicity.) The race/ethnicity categories considered are 'Non-Hispanic White', 'Non-Hispanic Black', 'Asian', 'Hispanic', and 'Other', which includes persons not categorized under the first four groups.

To process the census tract networks for each metropolitan area, we first map each census tract to its corresponding core-based Metropolitan Statistical Area (MSA) using the county designation of the tract. We then use TIGER shapefile data [32] for the census tracts to determine the network G = (V, E) of adjacent tracts in each MSA. Finally, the longitudinal ethnoracial distribution data is then mapped to the nodes in each network using the census tract IDs. To reduce noise as much as possible in our analysis, we kept only metros with at least 100 tracts that had complete ethnoracial distribution estimates in all tracts for the four decades 1980, 1990, 2000, and 2010. After preprocessing, 110 metro networks remained for the analysis in Sec. III C, one of which was the New Haven-Milford metro used for the case study in Sec. IIIB.

We make the tract adjacency networks for each metro we used in our analysis (with accompanying node metadata including ethnoracial distributions), as well as code for executing our algorithm publicly available at https: //github.com/aleckirkley/MDL_regionalization.

III. RESULTS

A. Cluster recovery in synthetic data

As a first test of our method, we explore its capability of recovering clusters in synthetic data. To do this, we create a synthetic model of spatial distributional data that has four tunable parameters: the number of clusters K, the number of covariate categories R, the level of statistical noise between the cluster-level distributions $\epsilon_{between}$, and the level of statistical noise within the clusters, ϵ_{within} . The model requires a spatial network G = (V, E) representing the adjacencies among spatial units (we use the census tract network for the New

Haven-Milford metropolitan area, see Sec. IIIB for details), although the specific choice of G does not tend to make a big qualitative difference in the results. It is also possible to include variable unit populations b(u) in this model, but for simplicity we set b(u) = 10000 for all $u \in V$ so that these values correspond roughly to the values seen in the real U.S. census tract data in Sec. IIIB and Sec. IIIC.

To generate a realization of the model, we first randomly partition the units into contiguous clusters by picking K units ("seeds") at random and constructing the Voronoi tesselation of the network with respect to these seeds. This Voronoi tesselation places each unit into the cluster corresponding to the seed geographically nearest to the unit, and in doing so guarantees that all clusters are contiguous. (This tesselation tends to produce relatively compact regions, but there are other reasonable alternative tesselations for generating the randomized contiguous partition.) We denote this "planted" partition $\mathcal{P}_{planted}$, to distinguish it from the partition \mathcal{P} inferred using our minimum description length algorithm.

Next, each cluster V_k is assigned a vector $\boldsymbol{x}(V_k)$ which tunes the covariate distributions within the units that comprise V_k . $\boldsymbol{x}(V_k)$ is drawn from a Dirichlet distribution with length-R concentration parameter $\alpha = \epsilon_{between}^{-1} \mathbf{1}_R$. This allows us to tune the level of differentiation between the cluster-level distributions, as well as the localization of these distributions. For low levels of betweencluster noise $\epsilon_{between}$, the distributions $\boldsymbol{x}(V_k)$ will all tend to distribute their probability relatively equally around the R categories, and there is little differentiation between the clusters V_k . On the other hand, for high levels of between-cluster noise $\epsilon_{between}$, there will be high between-cluster variance in the distributions $\{x(V_k)\}$, which will each tend to localize around a single category r. In general, the higher the between-cluster noise $\epsilon_{between}$ is, the easier it should be to recover the planted clusters in the synthetic data with our partitioning algorithm, since the clusters are more easily distinguished.

To tune the level of noise within each cluster V_k , we generate the distribution $x(u) = \{b_r(u)\}_{r=1}^R/b(u)$ for each $u \in V_k$ using $\boldsymbol{x}(u) = (1 - \epsilon_{within})\boldsymbol{x}(V_k) +$ $\epsilon_{within} \boldsymbol{x}_{noise}$, where \boldsymbol{x}_{noise} is drawn from a Dirichlet distribution with concentration parameters equal to 1. If the level of within-cluster noise ϵ_{within} is close to 0, then each x(u) for $u \in V_k$ will be roughly the same as $x(V_k)$, and thus the units within the cluster are highly homogeneous. On the other hand, if the level of within-cluster noise ϵ_{within} is close to 1, then the vectors $\boldsymbol{x}(u)$ will have high variability within the cluster V_k and contain little information about each other. As opposed to the between-cluster noise, higher values of the within-cluster noise ϵ_{within} correspond to it being harder to recover the planted clusters in the synthetic data, since the clusters are not as homogeneous in composition.

To measure the performance of our algorithm for any particular draw from the model, we compute the normalized mutual information [33] between our inferred

minimim description length partition \mathcal{P} and the planted partition $\mathcal{P}_{planted}$. The mutual information tells us how much information is shared between the two partitions, and its value is then normalized to fall in [0,1] so that 0 corresponds to completely uncorrelated partitions, and 1 corresponds to identical partitions (up to an arbitrary relabeling of the clusters). Letting $\mathcal{P} = \{V_k\}$ and $\mathcal{P}_{planted} = \{U_{k'}\}$, the mutual information $MI(\mathcal{P}, \mathcal{P}_{planted})$ is given by

$$MI(\mathcal{P}, \mathcal{P}_{planted}) = \sum_{k,k'} \frac{|V_k \cap U_{k'}|}{n(V)} \log \frac{n(V)|V_k \cap U_{k'}|}{|V_k||U_{k'}|}.$$
(11)

The mutual information can be normalized to fall in [0,1] by dividing by the average of the entropies of the individual partitions \mathcal{P} and $\mathcal{P}_{planted}$, giving

$$NMI(\mathcal{P}, \mathcal{P}_{planted}) = 2 \frac{MI(\mathcal{P}, \mathcal{P}_{planted})}{H(\mathcal{P}) + H(\mathcal{P}_{planted})}, \quad (12)$$

with

$$H(\mathcal{P}) = -\sum_{k} \frac{|V_k|}{n(V)} \log \frac{|V_k|}{n(V)} \tag{13}$$

and

$$H(\mathcal{P}_{planted}) = -\sum_{k'} \frac{|U_{k'}|}{n(V)} \log \frac{|U_{k'}|}{n(V)}.$$
 (14)

The normalized mutual information is a standard and well-tested measure for comparing partitions of networks [34, 35], but it has a critical shortcoming for our particular application in that it gives very high baseline values to completely random contiguous partitions of spatial networks. The reason for this is that Eq. 12 compares the partitions \mathcal{P} and $\mathcal{P}_{planted}$ relative to the ensemble of all possible partitions of the network, contiguous or not, and the constraint of contiguity induces a non-trivial level of correlation between the partitions. To correct for this, we rescale the normalized mutual information to the interval [0, 1] by subtracting off its minimum value over the range of ϵ_{within} values, and dividing by one minus this minimum value. It is then easy to see when we reach the NMI value at which the partitions are minimally correlated, subject to the contiguity constraint. Our rescaling does not map the highest value of the NMI over the ϵ_{within} range in each panel to 1, so that we have better differentiation of performance in the low noise region. Indeed, we will see that the zero-noise values of the rescaled NMI are slightly less than 1 in most cases, since some sampled model realizations will by chance produce some adjacent clusters that are nearly indistingushable.

In Fig. 2 we show the results of generating realizations of synthetic contiguous partitions from our model, and running our regionalization algorithm on each of these realizations to try to recover the planted clusters. Each data point represents the average rescaled normalized

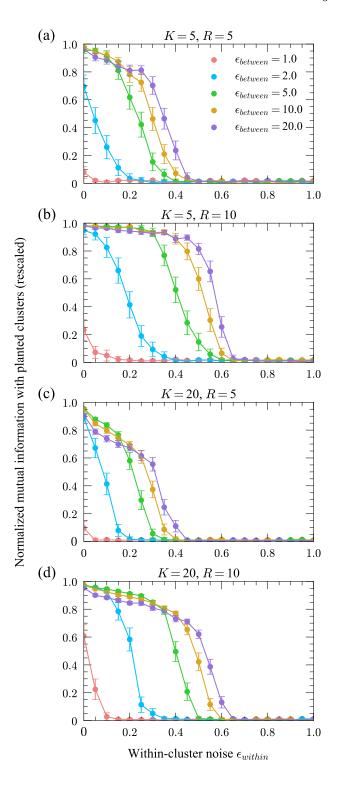


FIG. 2: Recovery of synthetic clusters generated by the model in Sec. III A. In each panel, the recovery performance of our algorithm, as measured by the $NMI(\mathcal{P}, \mathcal{P}_{planted})$ in Eq. 12 (rescaled to a zero baseline value) is plotted against the level of within-cluster noise ϵ_{within} , for various values of between-cluster noise $\epsilon_{between}$. The number of clusters K and the number of variable categories R are varied across the panels.

mutual information over 100 of these cluster recovery experiments, with error bars representing 2 standard errors. We can see that as the level of within-cluster noise ϵ_{within} increases, it becomes harder for us to recover the planted partition (as expected), but that we still have recovery better than the baseline value for levels of withincluster noise up to around $\epsilon_{within} \approx 0.4$ for R = 5 and $\epsilon_{within} \approx 0.7$ for R = 10. Recovery is better for R = 10than R=5, as it is less likely for the modes of the distributions $x(V_k)$ to overlap if R is larger. We can also observe that the recovery task becomes easier as $\epsilon_{between}$ and R increase, but how much easier it becomes depends on the number of clusters K. It becomes more likely that the highly concentrated cluster distributions $x(V_k)$ resulting from high $\epsilon_{between}$ have overlapping modes as K increases, and we thus see slightly worse recovery performance for high values of $\epsilon_{between}$ at K=20 than at K=5, since clusters will be harder to differentiate. In general, however, the performance of our algorithm is not terribly sensitive to the number of planted clusters, since we've varied K by a factor of 4 and only see a modest reduction in recovery performance.

Overall, the results of Figure 2 indicate that our minimum description length regionalization algorithm is able to successfully recover artificially planted clusters, even in the presence of substantial noise. We now move on to examine its performance on real ethnoracial distribution data.

B. Case study: Ethnoracial composition of the New Haven-Milford metropolitan area

To illustrate how the clusters obtained with our regionalization algorithm capture meaningful patterns in real data, we look at a case study of the ethnoracial evolution of the New Haven-Milford, Connecticut metropolitan area, using the data described in Sec. II C. This metro was chosen for the case study analysis due to its relatively high diversity, distinct spatial evolution for different ethnoracial groups, and low heterogeneity in census tract density in comparison with other small metros, allowing for a clear visual analysis of its temporal segregation patterns.

In Fig. 3, we show the evolution of the spatial distribution of ethnoracial groups, along with the regional boundaries inferred from minimizing the description length in Eq. 8, for the census tracts in the New Haven-Milford metro area between 1980 and 2010. Points are distributed randomly within each tract in proportion to the fraction of the population in each ethnoracial category. We can see that, in general, the clusters inferred through our algorithm correspond to heterogeneities in the spatial densities of these ethnoracial groups. The outlying tracts in the clusters, particularly in the year 2000, do not have as high a proportion of minority ethnoracial groups as the more densely packed areas of the clusters, but we can see these areas begin to fill out with minority populations

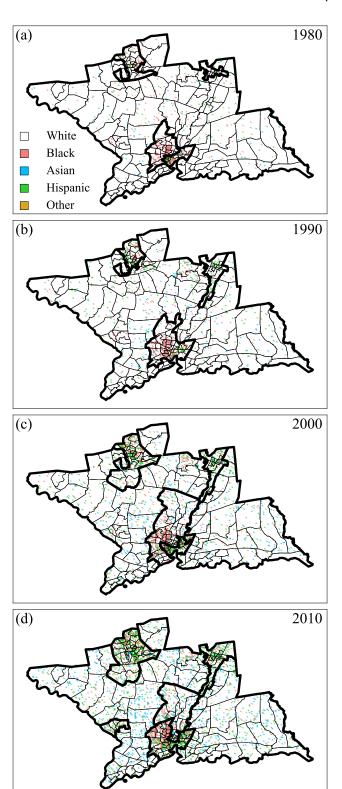


FIG. 3: Ethnoracial distributions in census tracts (thin black borders) within the New Haven-Milford, Connecticut metropolitan area, with inferred cluster boundaries from the minimum description length regionalization algorithm (thick black borders). Colored points are distributed at random within each tract and each color covers an area proportional to the fraction of the population within the tract that falls under the ethnoracial category corresponding to that color.

in 2010. (Their inclusion status in the cluster is determined by their slightly higher relative concentrations of the minority groups dominant in the core of their cluster, compared to nearby areas.)

Two emerging Black/Hispanic clusters in the north and one in the south are the predominant clusters captured by the algorithm, which assigns the rest of the metro to a single more rural/suburban and predominantly White cluster. We see that these clusters trend towards higher percentages of Hispanics relative to Non-Hispanic Blacks, which is consistent with the high influx of Latinos to the area between 1990 and 2000 [36]. The spatial extent of these Black/Hispanic clusters increases over time, reaching out into the less dense region of the metro that was predominantly White in 1980, which is consistent with 'White flight' during deindustrialization as well as the expanding influence of Yale University in the south [37]. In 2010, we see a slightly different configuration of clusters, with the northern Black/Hispanic clusters remaining largely in tact, but the southern-most cluster splitting into a largely Black/Hispanic cluster and one relatively mixed cluster. In 2000, this mixed cluster was merged with a primarily Black cluster, but in 2010 we can see that the movement of Hispanic population into the previously Black cluster provided a high enough level of Black/Hispanic mixing to create a single dense southern-most cluster, and a separate cluster to the north with smaller overall minority populations. In 2010 we also see the emergence of a new largely Hispanic cluster to the west.

In addition to the contributions Black/Hispanic clusters, the rural/suburban tracts diversified metro-wide due to an influx of Asian and Hispanic populations to the area [38]. For the most part these outlying tracts do not have sufficient differentiation in their ethnoracial distributions to necessitate separate clusters, and they are all grouped into a similar majority-White cluster for all four decades. However, this increasing overall diversity does result in greater difficulty compressing the data, as there is a clear positive trend in the inverse compression ratio η (Eq. 10) over the four decades, with $\eta = \{0.74, 0.77, 0.85, 0.87\}$ for {1980, 1990, 2000, 2010} respectively. We will show in the next section that a similar trend is seen across all the metros in our dataset, demonstrating the increasing complexity in urban segregation patterns country-wide.

C. Compression of ethnoracial data across metros

Now that we have demonstrated that our regionalization method is capable of identifying meaningful clusters in ethnoracial census data, we move on to a large scale analysis of the metro area networks described in Sec. II C. Specifically, we look at the extent to which the data within each metro can be compressed by our algorithm according to Eq. 10, which is an indicator of the overall complexity of the segregation patterns in these

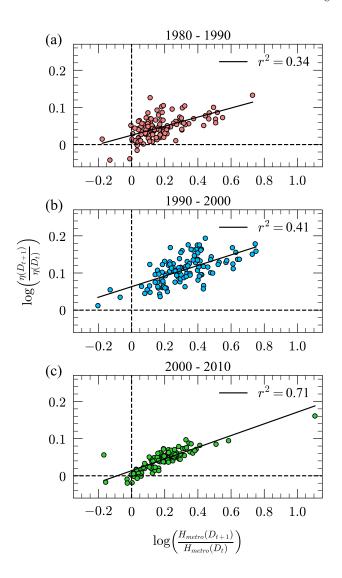


FIG. 4: Log-ratio of consecutive inverse compression ratios η (Eq. 10) versus the log-ratio of consecutive overall metro diversities H_{metro} (Eq. 15), in U.S. metros over the decades spanning t=1980 to t=2010. Dotted lines at x=0 and y=0 are displayed for reference, along with OLS regression lines (solid black) and their coefficients of determination r^2 . The slopes of all regression lines were highly statistically significant at the 0.01 significance level. Without grouping the changes by decade, we find $r^2=0.52$, and that the slope is again highly significant at the 0.01 significance level.

areas, as discussed in Sec. IIB.

From a purely visual analysis, one can easily argue that the segregation patterns seen in the New Haven-Milford metro in Fig. 3 are becoming more complex over time: describing to somebody the spatial distribution of ethnoracial groups in this metro would require more effort in 2010 than in 1980. And although this concept is a bit difficult to express in precise language due to the highly multifaceted nature of patterns in spatial data, we can capture this intuition through the inverse compres-

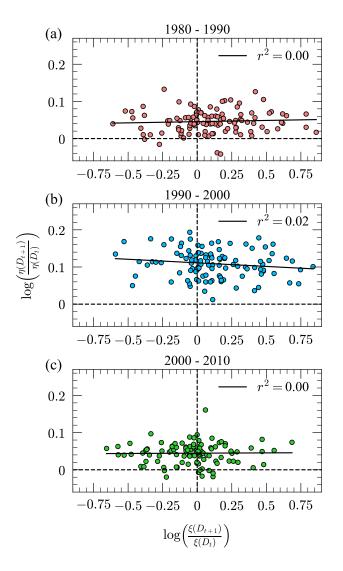


FIG. 5: Log-ratio of consecutive inverse compression ratios η (Eq. 10) versus the log-ratio of consecutive cluster scales ξ (Eq. 17), in U.S. metros over the decades spanning t=1980 to t=2010. None of the regression line slopes were statistically significant, even at the 0.10 significance level. Without grouping the changes by decade, we find $r^2=0.01$, and that the slope is again not significant at the 0.10 significance level.

sion ratio of Eq. 10, which tells us how efficiently we can compress the data for its exact description to a receiver. As discussed in Sec. III B, the inverse compression ratio $\eta(D)$ increases for the New Haven-Milford over the decades spanning 1980 to 2010.

Despite the difficulty we may have in succinctly discussing the overall complexity of the observed segregation patterns, there are a few key features that stand out in the plots of Fig. 3. The first is the increasing diversity of a typical tract in the metro area, demonstrated by a greater and greater fraction of area covered by colored points as time progresses. The second feature that stands out is the changing spatial extent of the clustered

areas, seen through the gradual absorption of the primarily White outlying tracts in 1980 into the minority-dense clusters as these clusters expand. In this section we explore the question of whether or not segregation patterns become more complex (as quantified by Eq. 10) in metros other than New Haven-Milford, and to what extent the patterns we observe across these metros are consistent with the features of overall diversity and changing spatial scales of clustering.

To measure the overall diversity of the data D in each metro area, the first feature of interest, we compute the entropy $H_{metro}(D)$ of the ethnoracial distribution obtained by aggregating all tract-level distributions in the metro, given by

$$H_{metro}(D) = -\sum_{r=1}^{R} P_r \log P_r, \tag{15}$$

where

$$P_r = \frac{\sum_{u \in V} b_r(u)}{b(V)} \tag{16}$$

is the fraction of the overall population in the metro that are classified under ethnoracial group r. Eq. 15 will take its minimum value of 0 when the population in D is concentrated entirely into a single category r, and its maximum value of $\log R$ when all categories have equal representation in the metro.

To measure the second feature of interest, the spatial scale of clustering for a metro area, we define the characteristic cluster scale $\xi(D)$ as

$$\xi(D) = \sqrt{\frac{\sum_{k} A(V_k)^2}{A(V)}},\tag{17}$$

where A(V') is the area of tracts in the subset $V' \subseteq V$, and $\mathcal{P} = \{V_k\}_{k=1}^K$ is the minimum description length partition of the metro. Eq. 17 will take its minimum value of $\sqrt{A(V)/n(V)}$ when each cluster has a spatial extent of A(V)/n(V)—the area of a single tract if the tracts were of equal size and each cluster only consisted of a single tract. Conversely, Eq. 17 will take its maximum value of $\sqrt{A(V)}$, the length scale of the entire metro, when the data D is best compressed with only a single cluster.

In Figures 4 and 5 we show how changes in the inverse compression ratio η (Eq. 10) correspond to changes in H_{metro} (Eq. 15) and ξ (Eq 17), across all 110 metros for each time period in our dataset (see Sec. II C for details on the dataset). In order to identify statistical associations between the variables, while removing temporal trends and accounting for potentially nonlinear dependencies, ordinary least squares (OLS) regression analysis was performed on the differences in the logarithm of each quantity over each of the periods 1980–1990, 1990–2000, and 2000-2010 (panels (a), (b), and (c) respectively in each of the figures). All significance results reported in the captions hold up under Bonferroni correction for multiple comparisons [39].

We can see that the inverse compression ratio η is in general increasing over all time periods, as the majority of the points in both figures fall above the line y=0 (the y-axes are the same in Figures 4 and 5). In particular, the values of η increased substantially between t=1990 and t=2000, with all metros in our dataset having a positive change in this quantity during this decade. This general pattern of increasing compressibility, with the greatest change occurring during the 1990-2000 period, is consistent with the case study analysis in Sec. III B.

Looking at Fig. 4, we can observe a consistently increasing level of overall diversity in the metro areas, as illustrated by the majority of points falling above the line x = 0 in the three plots. This observation is consistent with findings that suburbs have generally become more racially diverse [40], and that there are an increasing number of "no-majority" communities in which no ethnoracial group makes up more than half of the population [41]. The Scranton Wilkes-Barre metro area represents a clear outlier regarding changes in overall diversity, as its value of H_{metro} shot up in 2010, with roughly a 116% increase from relatively low values in the first three decades. The coefficients of determination r^2 for the regression analyses reveal that the temporal changes in H_{metro} are highly correlated with the changes in η over the same time periods, with the strongest correlation occurring between 2000 and 2010. These r^2 values, along with the statistically significant p-values of the corresponding regression line slopes (all of which had $p \ll 0.01$), suggest that the overall diversity of metros is an important factor for determining the complexity in segregation patterns we see according to Eq. 10.

In Fig. 5, we observe no clear trend in the changes in the characteristic cluster length scales ξ across metros for each time period, with roughly half of the metros in each time period having decreasing values ξ , and half having increasing values of ξ . The metros that comprise these two halves also differ across time periods: only 18 of the 110 metros studied had monotonically increasing or decreasing values of ξ across all time periods (compared to 103 of 110 metros having a value of H_{metro} that increased throughout all decades). The r^2 values for the regression analyses in Fig. 5 indicate that the temporal changes in ξ are poorly correlated with the changes in η over the same time periods, with r^2 values in two of the decades even rounding to 0 up to two decimal places. The p-values corresponding to the slopes of the regression lines plotted do not indicate any statistically significant linear relationship between the plotted variables—p = 0.52, 0.13,and 0.89 for panels (a), (b), and (c) respectively. These results suggest that the increasing complexity of segregation patterns we observe across metros is not substantially affected by the characteristic spatial scale at which the tracts can be optimally clustered in each metro (at least when considering census tracts as the fundamental

unit, which may blur out segregation patterns at even smaller scales [42]).

Altogether, this analysis indicates that segregation patterns in large U.S. metros are becoming more complex over time, as the ethnoracial data in these areas is becoming more difficult to compress. The overall diversification of these metros plays an important role in increasing the complexity of these segregation patterns, while the manifestation of increasingly granular spatial clustering among ethnoracial groups is likely not a major contributor.

IV. CONCLUSION

Here we have presented a regionalization algorithm based on the minimum description length principle for partitioning a set of spatial units with distributional metadata into contiguous clusters. Our method requires no user input, learning the natural clusters that result in a maximally compressed representation of the data. We demonstrate that our approach can effectively recover synthetically planted clusters in noisy spatial data, and that it returns a useful partitioning of ethnoracial census data in U.S. metropolitan areas. We uncover new insights about the ethnoracial segregation patterns in these U.S. metros using our methodology, finding that these patterns have become increasingly complex over time, in part due to the increasing ethnoracial diversity of the metros over the time period studied.

There are a number of ways our method can be extended in future work. Our current formulation requires the spatial data of interest to take the form of a single discrete set of counts within each unit, but it may be possible to adapt our description length calculation to multiple spatial covariates simultaneously, or to ordinal or continuous distributions. This would allow us to perform regionalization with respect to a variety of attributes of interest with variable data types, for example race and income, all at once. It is also possible to include additional penalties in the regionalization objective function we use for clustering, to enforce constraints on the size, shape, or populations of the clusters, which may make it more suitable for policy-driven applications of regionalization. Extension of our transmission procedure to a multi-step, hierarchical encoding scheme may also prove useful, as this would allow for multiscalar regionalization.

Acknowledgments: The author thanks Mark Newman for useful discussions regarding the use of mutual information for spatial clustering, and Phil Chodrow for useful discussions about the data. This work was funded by the US Department of Defense NDSEG fellowship program.

- M. Fujita, P. R. Krugman, and A. Venables, The Spatial Economy: Cities, Regions, and International Trade. MIT press, Cambridge, MA (1999).
- [2] L. A. Brown and S.-Y. Chung, Spatial segregation, segregation indices and the geographical perspective. *Population, Space and Place* 12, 125–143 (2006).
- [3] P. Legendre and M. J. Fortin, Spatial pattern and ecological analysis. Vegetatio 80, 107–138 (1989).
- [4] S. E. Spielman and D. C. Folch, Reducing uncertainty in the American Community Survey through data-driven regionalization. PLOS One 10, e0115626 (2015).
- [5] S. E. Spielman and A. Singleton, Studying neighborhoods using uncertain data from the American Community Survey: A contextual approach. *Annals of the Association* of American Geographers 105, 1003–1025 (2015).
- [6] M. M. Rahman, Regionalization of urbanization and spatial development: Planning regions in Bangladesh. *The Journal of Geo-Environment* 4, 31–46 (2004).
- [7] R. Fovell and M. Fovell, Climate zones of the conterminous United States defined using cluster analysis. *Journal of Climate* 6, 2103–2135 (1993).
- [8] M. Garreton and R. Sanchez, Identifying an optimal analysis level in multiscalar regionalization: A study case of social distress in Greater Santiago. Computers, Environment and Urban Systems 56, 14–24 (2016).
- [9] H. Peterson, J. Nieber, and R. Kanivetsky, Hydrologic regionalization to assess anthropogenic changes. *Journal* of Hydrology 408, 212–225 (2011).
- [10] J. Niesterowicz, T. F. Stepinski, and J. Jasiewicz, Unsupervised regionalization of the United States into land-scape pattern types. *International Journal of Geographical Information Science* 30, 1450–1468 (2016).
- [11] J. A. George, B. W. Lamar, and C. A. Wallace, Political district determination using large-scale network optimization. *Socio-Economic Planning Sciences* 31, 11–28 (1997).
- [12] J. C. Duque, R. Ramos, and J. Suriñach, Supervised regionalization methods: A survey. *International Regional* Science Review 30, 195–220 (2007).
- [13] W. Li, M. F. Goodchild, and R. Church, An efficient measure of compactness for two-dimensional shapes and its application in regionalization problems. *International Journal of Geographical Information Science* 27, 1227– 1250 (2013).
- [14] R. M. Assunção, M. C. Neves, G. Câmara, and C. da Costa Freitas, Efficient regionalization techniques for socioeconomic geographical units using minimum spanning trees. *International Journal of Geographical In*formation Science 20, 797–811 (2006).
- [15] R. Wei, S. Rey, and E. Knaap, Efficient regionalization for spatially explicit neighborhood delineation. *Interna*tional Journal of Geographical Information Science 35, 135–151 (2021).
- [16] O. Aydin, M. V. Janikas, R. M. Assunção, and T.-H. Lee, A quantitative comparison of regionalization methods. *International Journal of Geographical Information* Science 35, 2287–2315 (2021).
- [17] J. C. Duque, L. Anselin, and S. J. Rey, The max-pregions problem. *Journal of Regional Science* 52, 397– 419 (2012).
- [18] R. Wright, M. Ellis, S. R. Holloway, and S. Wong, Pat-

- terns of racial diversity and segregation in the United States: 1990–2010. The Professional Geographer 66, 173–182 (2014).
- [19] M. Olteanu, J. Randon-Furling, and W. A. Clark, Segregation through the multiscalar lens. *Proceedings of the National Academy of Sciences* 116, 12250–12254 (2019).
- [20] A. Grainger, The role of spatial scale and spatial interactions in sustainable development. In Exploring Sustainable Development: Geographical Perspectives, Earthscan, London (2004).
- [21] A. Kirkley, Information theoretic network approach to socioeconomic correlations. *Physical Review Research* 2, 043212 (2020).
- [22] P. D. Grünwald and A. Grünwald, The Minimum Description Length Principle. MIT Press, Cambridge, MA (2007).
- [23] T. M. Cover and J. A. Thomas, Elements of Information Theory. John Wiley & Sons, Hoboken (2012).
- [24] T. Li, S. Ma, and M. Ogihara, Entropy-based criterion in categorical clustering. In *Proceedings of the Twenty-first International Conference on Machine Learning*, p. 68, Association for Computing Machinery, New York (2004).
- [25] O. Georgieva, K. Tschumitschew, and F. Klawonn, Cluster validity measures based on the minimum description length principle. In *Proceedings of the International Conference on Knowledge-Based and Intelligent Information and Engineering Systems*, pp. 82–89, Springer-Verlag, Berlin (2011).
- [26] A. Kirkley and M. E. J. Newman, Representative community divisions of networks. Preprint arXiv:2105.04612 (2021).
- [27] M. Rosvall and C. T. Bergstrom, An information-theoretic framework for resolving community structure in complex networks. *Proceedings of the National Academy of Sciences* **104**, 7327–7331 (2007).
- [28] P. S. Chodrow, Structure and information in spatial segregation. Proceedings of the National Academy of Sciences 114, 11591–11596 (2017).
- [29] M. E. J. Newman, G. T. Cantwell, and J.-G. Young, Improved mutual information measure for clustering, classification, and community detection. *Physical Review E* 101, 042304 (2020).
- [30] D. S. Massey and N. A. Denton, The dimensions of residential segregation. Social Forces 67, 281–315 (1988).
- [31] J. R. Logan, Z. Xu, and B. J. Stults, Interpolating US decennial census tract data from as early as 1970 to 2010: A longitudinal tract database. The Professional Geographer 66, 412–420 (2014).
- [32] US Census Bureau, Tiger/line shapefiles (2019).
- [33] N. X. Vinh, J. Epps, and J. Bailey, Information theoretic measures for clusterings comparison: Variants, properties, normalization and correction for chance. *The Jour*nal of Machine Learning Research 11, 2837–2854 (2010).
- [34] L. Danon, J. Duch, A. Diaz-Guilera, and A. Arenas, Comparing community structure identification. *Journal* of Statistical Mechanics: Theory and Experiment 2005, P09008 (2005).
- [35] A. Lancichinetti, S. Fortunato, and F. Radicchi, Benchmark graphs for testing community detection algorithms. Physical Review E 78, 046110 (2008).
- [36] D. W. Vasquez, Latinos in New Haven, Connecticut.

- Research Report Gastón Institute Publications, No. 57 (2003).
- [37] M. D. Leonardo, There's no place like home: Domestic domains and urban imaginaries in New Haven, Connecticut. *Identities: Global Studies in Culture and Power* 113, 33–52 (2006).
- [38] M. Buchanan and M. Abraham, Understanding the impact of immigration in Greater New Haven. Research Report Community Foundation for Greater New Haven (2015).
- [39] R. G. Miller, Simultaneous Statistical Inference. Springer

- Verlag, New York (1981).
- [40] M. Orfield and T. F. Luce, America's racially diverse suburbs: Opportunities and challenges. *Housing Policy Debate* 23, 395–430 (2013).
- [41] C. R. Farrell and B. A. Lee, No-majority communities: Racial diversity and change at the local level. *Urban Affairs Review* 54, 866–897 (2018).
- [42] D. J. Krupka, Are big cities more segregated? Neighbour-hood scale and the measurement of segregation. *Urban Studies* 44, 187–197 (2007).